Extraction of the Weak Mixing Angle at the EIC

Michael Nycz

Alexander Emmert, and Xiaochao Zheng and the SMEFT group

CFNS Workshop: High Luminosity-EIC
June 21-24 2022

Work supported by DOE grant DE-SC0014434

Neutral-Current Electroweak Physics and SMEFT Studies at the EIC

Radja Boughezal[1], Alexander Emmert[2], Tyler Kutz[3], Sonny Mantry[4], Michael Nycz[2], Frank Petriello[1,5], Kağan Şimşek[5], Daniel Wiegand[5], Xiaochao Zheng[2]

[1] *Argonne National Laboratory, Lemont, IL, USA*
[2] *University of Virginia, Charlottesville, VA, USA*
[3] *Massachusetts Institute of Technology, Cambridge, MA, USA*
[4] *University of North Georgia, Dahlonega, GA, USA*
[5] *Northwestern University, Evanston, IL, USA*

We study the potential for precision electroweak (EW) measurements and beyond-the-Standard Model (BSM) searches using cross-section asymmetries in neutral-current (NC) deep inelastic scattering at the electron-ion collider (EIC). Our analysis uses a complete and realistic accounting of systematic errors from both theory and experiment and considers the potential of both proton and deuteron beams for a wide range of energies and luminosities. We also consider what can be learned from a possible future positron beam and a potential ten-fold luminosity upgrade of the EIC beyond its initial decade of running. We use the SM effective field theory (SMEFT) framework to parameterize BSM effects and focus on semi-leptonic four-fermion operators, whereas for our precision EW study, we determine how well the EIC can measure the weak mixing angle. New features of our study include the use of an up-to-date detector design of EIC Comprehensive Chromodynamics Experiment (ECCE) and accurate running conditions of the EIC, the simultaneous fitting of beam polarization uncertainties and Wilson coefficients to improve the sensitivity to SMEFT operators, and the inclusion of the weak mixing angle running in our fit template. We find that the EIC can probe BSM operators at scales competitive with and in many cases exceeding LHC Drell-Yan bounds while simultaneously not suffering from degeneracies between Wilson coefficients.

Neutral-Current Electroweak Physics and SMEFT Studies at the EIC

Neutral-Current Electroweak Physics and SMEFT Studies at the EIC

Radja Boughezal[1], Alexander Emmert[2], Tyler Kutz[3], Sonny Mantry[4], Michael Nycz[2], Frank Petriello[1,5], Kağan Şimşek[5], Daniel Wiegand[5], Xiaochao Zheng[2]

[1] *Argonne National Laboratory, Lemont, IL, USA*
[2] *University of Virginia, Charlottesville, VA, USA*
[3] *Massachusetts Institute of Technology, Cambridge, MA, USA*
[4] *University of North Georgia, Dahlonega, GA, USA*
[5] *Northwestern University, Evanston, IL, USA*

We study the potential for precision electroweak (EW) measurements and beyond-the-Standard Model (BSM) searches using cross-section asymmetries in neutral-current (NC) deep inelastic scattering at the electron-ion collider (EIC). Our analysis uses a complete and realistic accounting of systematic errors from both theory and experiment and considers the potential of both proton and deuteron beams for a wide range of energies and luminosities. We also consider what can be learned from a possible future positron beam and a potential ten-fold luminosity upgrade of the EIC beyond its initial decade of running. We use the SM effective field theory (SMEFT) framework to parameterize BSM effects and focus on semi-leptonic four-fermion operators, whereas for our precision EW study, we determine how well the EIC can measure the weak mixing angle. New features of our study include the use of an up-to-date detector design of EIC Comprehensive Chromodynamics Experiment (ECCE) and accurate running conditions of the EIC, the simultaneous fitting of beam polarization uncertainties and Wilson coefficients to improve the sensitivity to SMEFT operators, and the inclusion of the weak mixing angle running in our fit template. We find that the EIC can probe BSM operators at scales competitive with and in many cases exceeding LHC Drell-Yan bounds while simultaneously not suffering from degeneracies between Wilson coefficients.

Neutral-Current Electroweak Physics and SMEFT Studies at the EIC

Weak Mixing Angle Measurement at EIC

- Main focus of EIC is on exploring fundamental QCD
  - Can also have an impact on Electroweak and BSM physics
  - Discussed in Yellow Report
- The EIC can provide constraints on $\sin^2\theta_W$ over a wide Q^2 range
  - Energy range between those achievable in fixed-target and collider experiments
- Proton target?
  - PVDIS experiments extracting $\sin^2\theta_W$ focus on the isoscalar deuteron due to cancelation of structure function effects
  - High precision data at EIC may make extraction of $\sin^2\theta_W$ from the proton*EIC Yellow Report
- **Both deuteron and proton beams used in the following study**
- **Analysis uses realistic uncertainties for both theoretical and experimental systematics to determine impact of EIC on $\sin^2\theta_W$**

Parity Violating Asymmetry

- PVDIS asymmetry:
  1. $A_{\mathrm{PV}}^{(e)} \equiv \frac{\sigma_R - \sigma_L}{\sigma_R + \sigma_L} = \frac{d\sigma_e}{d\sigma_0}$ (unpolarized)
     - $\sigma_R(\sigma_L)$ is the cross-section of right-handed (left-handed) electrons scattering off unpolarized hadrons
  2. $A_{\mathrm{PV}}^{(H)} \equiv \frac{d\sigma_H}{d\sigma_0}$ (polarized)
     - Unpolarized e⁻ scattering off of right-handed and left-handed hadrons

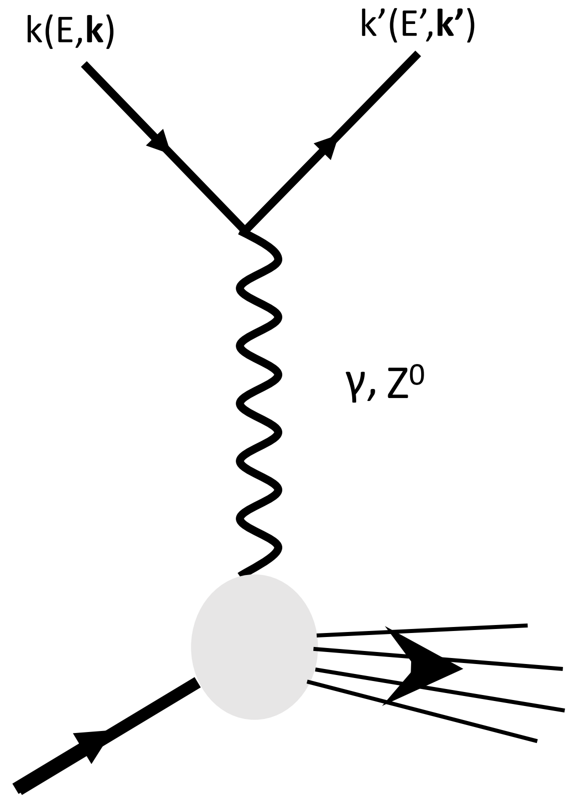

Parity Violating Asymmetry

- PVDIS asymmetry:
  1. $A_{\rm PV}^{(e)} \equiv \frac{\sigma_R - \sigma_L}{\sigma_R + \sigma_L} = \frac{d\sigma_e}{d\sigma_0}$ (unpolarized)
  - $\sigma_R(\sigma_L)$ is the cross-section of right-handed (left-handed) electrons scattering off unpolarized hadrons
  2. $A_{\rm PV}^{(H)} \equiv \frac{d\sigma_H}{d\sigma_0}$ (polarized)
  - Unpolarized e^- scattering off of right-handed and left-handed hadrons

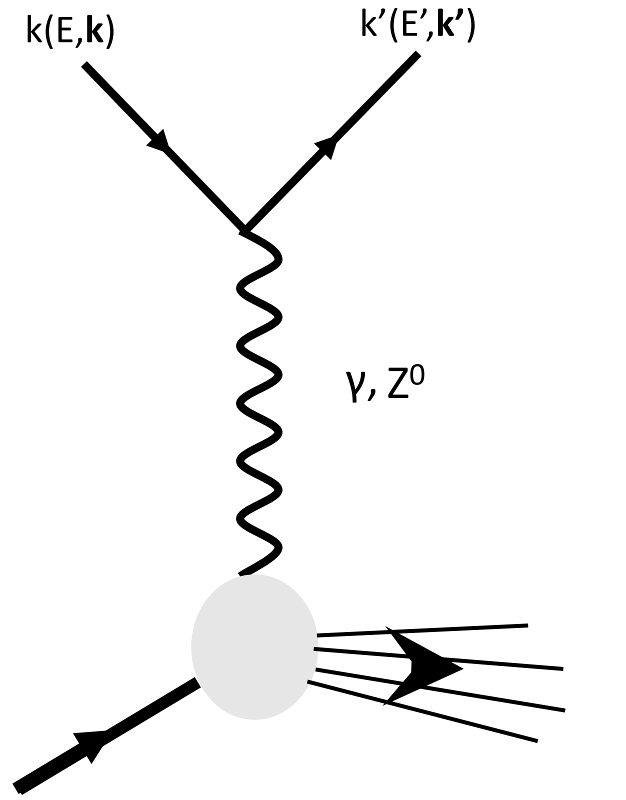

Neutral Current Electroweak Physics Studies at the EIC

DIS cross sections: $d\sigma = d\sigma_0 + P_e d\sigma_e + P_H d\sigma_H + P_e P_H d\sigma_{eH}$

$$d\sigma_0 = \frac{1}{4}\Big[d\sigma|_{\lambda_e=+1,\lambda_H=+1} + d\sigma|_{\lambda_e=+1,\lambda_H=-1} + d\sigma|_{\lambda_e=-1,\lambda_H=+1} + d\sigma|_{\lambda_e=-1,\lambda_H=-1}\Big],$$
$$d\sigma_e = \frac{1}{4}\Big[d\sigma|_{\lambda_e=+1,\lambda_H=+1} + d\sigma|_{\lambda_e=+1,\lambda_H=-1} - d\sigma|_{\lambda_e=-1,\lambda_H=+1} - d\sigma|_{\lambda_e=-1,\lambda_H=-1}\Big],$$
$$d\sigma_H = \frac{1}{4}\Big[d\sigma|_{\lambda_e=+1,\lambda_H=+1} - d\sigma|_{\lambda_e=+1,\lambda_H=-1} + d\sigma|_{\lambda_e=-1,\lambda_H=+1} - d\sigma|_{\lambda_e=-1,\lambda_H=-1}\Big],$$
$$d\sigma_{eH} = \frac{1}{4}\Big[d\sigma|_{\lambda_e=+1,\lambda_H=+1} - d\sigma|_{\lambda_e=+1,\lambda_H=-1} - d\sigma|_{\lambda_e=-1,\lambda_H=+1} + d\sigma|_{\lambda_e=-1,\lambda_H=-1}\Big],$$

$$\frac{d^2\sigma_0}{dxdy} = \frac{4\pi\alpha^2}{xyQ^2}\Big\{(1-y)\Big[F_2^\gamma - g_V^e \eta_{\gamma Z} F_2^{\gamma Z} + (g_V^{e\,2} + g_A^{e\,2})\eta_Z F_2^Z\Big] + xy^2\Big[F_1^\gamma - g_V^e \eta_{\gamma Z} F_1^{\gamma Z} + (g_V^{e\,2} + g_A^{e\,2})\eta_Z F_1^Z\Big] - \frac{xy}{2}(2-y)\Big[g_A^e \eta_{\gamma Z} F_3^{\gamma Z} - 2 g_V^e g_A^e \eta_Z F_3^Z\Big]\Big\},$$

$$\frac{d^2\sigma_e}{dxdy} = \frac{4\pi\alpha^2}{xyQ^2}\Big\{(1-y)\Big[g_A^e \eta_{\gamma Z} F_2^{\gamma Z} - 2 g_V^e g_A^e \eta_Z F_2^Z\Big] + xy^2\Big[g_A^e \eta_{\gamma Z} F_1^{\gamma Z} - 2 g_V^e g_A^e \eta_Z F_1^Z\Big] + \frac{xy}{2}(2-y)\Big[g_V^e \eta_{\gamma Z} F_3^{\gamma Z} - (g_V^{e\,2} + g_A^{e\,2})\eta_Z F_3^Z\Big]\Big\},$$

$$\frac{d^2\sigma_H}{dxdy} = \frac{4\pi\alpha^2}{xyQ^2}\Big\{(2-y)\,xy\Big[g_A^e \eta_{\gamma Z} g_1^{\gamma Z} - 2 g_V^e g_A^e \eta_Z g_1^Z\Big] - (1-y)\Big[-g_V^e \eta_{\gamma Z} g_4^{\gamma Z} + (g_V^{e\,2} + g_A^{e\,2})\eta_Z g_4^Z\Big] - xy^2\Big[-g_V^e \eta_{\gamma Z} g_5^{\gamma Z} + (g_V^{e\,2} + g_A^{e\,2})\eta_Z g_5^Z\Big]\Big\},$$

$$\frac{d^2\sigma_{eH}}{dxdy} = \frac{4\pi\alpha^2}{xyQ^2}\Big\{(2-y)\,xy\Big[g_1^\gamma - g_V^e \eta_{\gamma Z} g_1^{\gamma Z} + (g_V^{e\,2} + g_A^{e\,2})\eta_Z g_1^Z\Big] - (1-y)\Big[g_A^e \eta_{\gamma Z} g_4^{\gamma Z} - 2 g_V^e g_A^e \eta_Z g_4^Z\Big] + xy^2\Big[g_A^e \eta_{\gamma Z} g_5^{\gamma Z} - 2 g_V^e g_A^e \eta_Z g_5^Z\Big]\Big\}.$$

Parity-Violating asymmetries:

$$A_{PV}^{(e)} \equiv \frac{d\sigma_e}{d\sigma_0} \qquad A_{PV}^{(H)} \equiv \frac{d\sigma_H}{d\sigma_0}$$

Double-spin asymmetries:

$$A_{PV}^{(eH)} \equiv \frac{d\sigma_{eH}}{d\sigma_0}$$

Lepton-charge asymmetries:

$$A_{LC,H} \equiv \frac{d\sigma_0^{e+} - d\sigma_0^{e-}}{d\sigma_0^{e+} + d\sigma_0^{e-}}$$

Neutral Current Electroweak Physics Studies at the EIC

DIS cross sections: $d\sigma = d\sigma_0 + P_e d\sigma_e + P_H d\sigma_H + P_e P_H d\sigma_{eH}$

$$d\sigma_0 = \frac{1}{4}\Big[d\sigma|_{\lambda_e=+1,\lambda_H=+1} + d\sigma|_{\lambda_e=+1,\lambda_H=-1} + d\sigma|_{\lambda_e=-1,\lambda_H=+1} + d\sigma|_{\lambda_e=-1,\lambda_H=-1} \Big],$$
$$d\sigma_e = \frac{1}{4}\Big[d\sigma|_{\lambda_e=+1,\lambda_H=+1} + d\sigma|_{\lambda_e=+1,\lambda_H=-1} - d\sigma|_{\lambda_e=-1,\lambda_H=+1} - d\sigma|_{\lambda_e=-1,\lambda_H=-1} \Big],$$
$$d\sigma_H = \frac{1}{4}\Big[d\sigma|_{\lambda_e=+1,\lambda_H=+1} - d\sigma|_{\lambda_e=+1,\lambda_H=-1} + d\sigma|_{\lambda_e=-1,\lambda_H=+1} - d\sigma|_{\lambda_e=-1,\lambda_H=-1} \Big],$$
$$d\sigma_{eH} = \frac{1}{4}\Big[d\sigma|_{\lambda_e=+1,\lambda_H=+1} - d\sigma|_{\lambda_e=+1,\lambda_H=-1} - d\sigma|_{\lambda_e=-1,\lambda_H=+1} + d\sigma|_{\lambda_e=-1,\lambda_H=-1} \Big],$$

Parity-Violating asymmetries:

$$A_{PV}^{(e)} \equiv \frac{d\sigma_e}{d\sigma_0} \qquad A_{PV}^{(H)} \equiv \frac{d\sigma_H}{d\sigma_0}$$

Double-spin asymmetries:

$$A_{PV}^{(eH)} \equiv \frac{d\sigma_{eH}}{d\sigma_0}$$

Lepton-charge asymmetries:

$$A_{LC,H} \equiv \frac{d\sigma_0^{e+} - d\sigma_0^{e-}}{d\sigma_0^{e+} + d\sigma_0^{e-}}$$

$$\begin{aligned}\frac{d^2\sigma_0}{dxdy} = \frac{4\pi\alpha^2}{xyQ^2}\Big\{ &(1-y)\left[F_2^\gamma - g_V^e\eta_{\gamma Z}F_2^{\gamma Z} + (g_V^{e\,2} + g_A^{e\,2})\eta_Z F_2^Z\right] \\ &+ xy^2\left[F_1^\gamma - g_V^e\eta_{\gamma Z}F_1^{\gamma Z} + (g_V^{e\,2} + g_A^{e\,2})\eta_Z F_1^Z\right] \\ &- \frac{xy}{2}(2-y)\left[g_A^e\eta_{\gamma Z}F_3^{\gamma Z} - 2g_V^e g_A^e \eta_Z F_3^Z\right]\Big\} ,\end{aligned}$$

$$\begin{aligned}\frac{d^2\sigma_e}{dxdy} = \frac{4\pi\alpha^2}{xyQ^2}\Big\{ &(1-y)\left[g_A^e\eta_{\gamma Z}F_2^{\gamma Z} - 2g_V^e g_A^e\eta_Z F_2^Z\right] + xy^2\left[g_A^e\eta_{\gamma Z}F_1^{\gamma Z} - 2g_V^e g_A^e\eta_Z F_1^Z\right] \\ &+ \frac{xy}{2}(2-y)\left[g_V^e\eta_{\gamma Z}F_3^{\gamma Z} - (g_V^{e\,2} + g_A^{e\,2})\eta_Z F_3^Z\right]\Big\} ,\end{aligned}$$

$$\begin{aligned}\frac{d^2\sigma_H}{dxdy} = \frac{4\pi\alpha^2}{xyQ^2}\Big\{ &(2-y)\,xy\left[g_A^e\eta_{\gamma Z}g_1^{\gamma Z} - 2g_V^e g_A^e\eta_Z g_1^Z\right] \\ &- (1-y)\left[-g_V^e\eta_{\gamma Z}g_4^{\gamma Z} + (g_V^{e\,2} + g_A^{e\,2})\eta_Z g_4^Z\right] \\ &- xy^2\left[-g_V^e\eta_{\gamma Z}g_5^{\gamma Z} + (g_V^{e\,2} + g_A^{e\,2})\eta_Z g_5^Z\right]\Big\} ,\end{aligned}$$

$$\begin{aligned}\frac{d^2\sigma_{eH}}{dxdy} = \frac{4\pi\alpha^2}{xyQ^2}\Big\{ &(2-y)\,xy\left[g_1^\gamma - g_V^e\eta_{\gamma Z}g_1^{\gamma Z} + (g_V^{e\,2} + g_A^{e\,2})\eta_Z g_1^Z\right] \\ &- (1-y)\left[g_A^e\eta_{\gamma Z}g_4^{\gamma Z} - 2g_V^e g_A^e\eta_Z g_4^Z\right] + xy^2\left[g_A^e\eta_{\gamma Z}g_5^{\gamma Z} - 2g_V^e g_A^e\eta_Z g_5^Z\right]\Big\} .\end{aligned}$$

Parity Violating Asymmetry

$$A_{RL}^{e^-} = \frac{|\lambda|\eta_{\gamma Z}\left[g_A^e 2yF_1^{\gamma Z} + g_A^e\left(\frac{2}{xy} - \frac{2}{x} - \frac{2M^2xy}{Q^2}\right)F_2^{\gamma Z} + g_V^e(2-y)F_3^{\gamma Z}\right]}{2yF_1^{\gamma} + \left(\frac{2}{xy} - \frac{2}{x} - \frac{2M^2xy}{Q^2}\right)F_2^{\gamma} - \eta_{\gamma Z}\left[g_V^e 2yF_1^{\gamma Z} + g_V^e\left(\frac{2}{xy} - \frac{2}{x} - \frac{2M^2xy}{Q^2}\right)F_2^{\gamma Z} + g_A^e(2-y)F_3^{\gamma Z}\right]}$$

Where

$$\left[F_2^{\gamma}, F_2^{\gamma z}, F_2^{z}\right] = x\sum_q [e_q^2, 2e_q\, g_V^q, \left(g_V^q\right)^2 + \left(g_A^q\right)^2](q + \bar{q})$$

$$\left[F_3^{\gamma}, F_3^{\gamma z}, F_3^{z}\right] = x\sum_q [0, 2e_q g_A^q, 2g_V^q g_A^q](q - \bar{q})$$

$$g_A^e = -\frac{1}{2} \qquad g_A^q = \pm\frac{1}{2}$$

$$g_V^e = -\frac{1}{2} + 2\sin^2\theta_W \qquad g_V^q = \pm\frac{1}{2} - 2e_q\sin^2\theta_W$$

$$\eta_{\gamma Z} = \frac{G_F Q^2}{2\sqrt{2}\pi\alpha}\frac{M_Z^2}{M_Z^2 + Q^2}$$

$g_A^{e(q)}$ and $g_V^{e(q)}$: axial and vector neutral weak couplings of the electron (quark)

Data sets simulated and processed

ep				*ed*		
Electron Energy [GeV]	Proton Energy [GeV]	Annual Luminosity [fb^{-1}]		Electron Energy [GeV]	Deuteron Energy [GeV]	Annual Luminosity [fb^{-1}]
5	41	4.4		5	41	4.4
5	100	36.8		5	100	36.8
10	100	44.8		10	100	44.8
10	275	100		10	137	100
18	275	15.4		18	137	15.4
18	275	100				

EIC Yellow Report Setting

$\sin^2\theta_W$ extracted from each of the pseudo-data sets

Neutral Current Electroweak Physics Studies at the EIC

Simulation:

- July 2021 concept, Djangoh 4.6.16 combined with fast-smearing from single-electron gun simulation
- Modified user routine of Djangoh to calculate counts and size of Apv
- Events unfolded to leptonic truth using R-matrix inversion method
  - **Best way to treat the uncertainty of unfolding and bin migration?**
- 20M events per energy/beam setting
- Inclusive electrons detected and identified by EIC Comprehensive Chromodynamics Experiment detector concept (ECCE) tracking and Ecal system

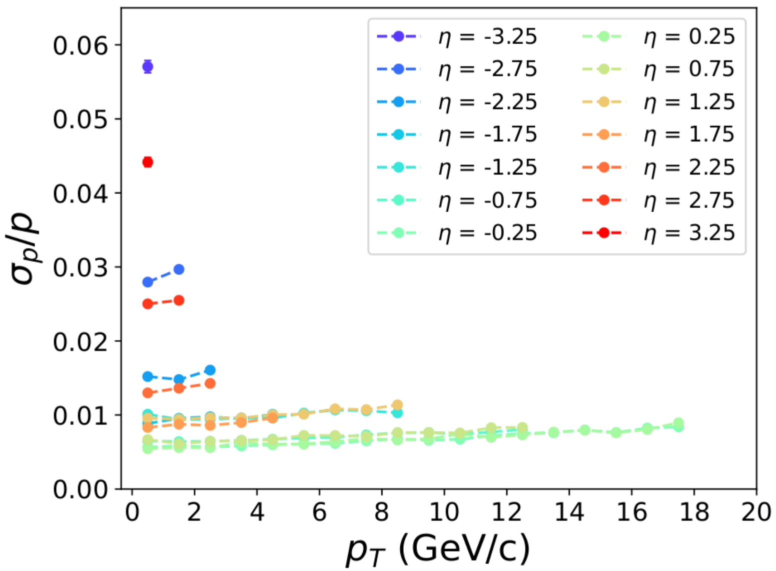

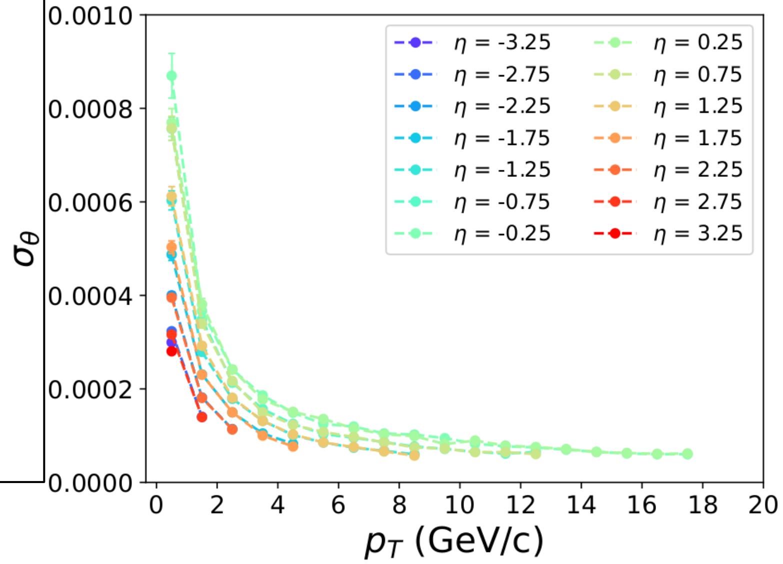

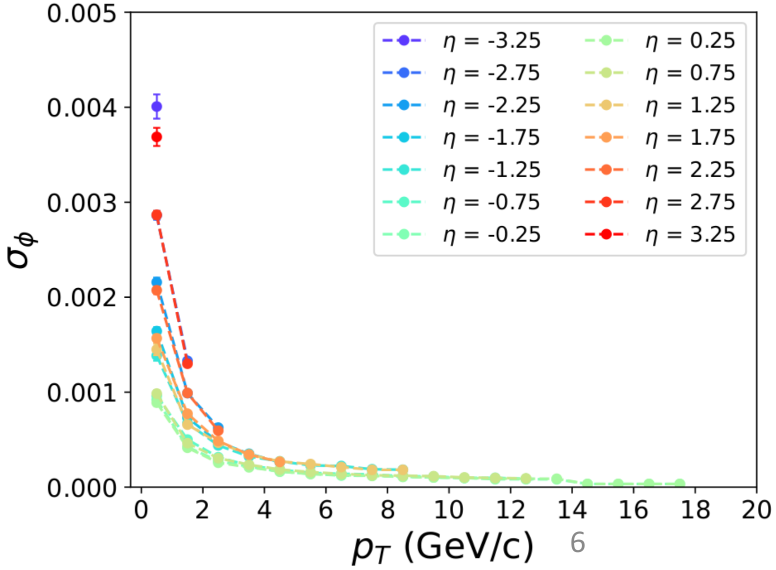

Neutral Current Electroweak Physics Studies at the EIC

Simulation:

Fast-smearing performed on:

- Electron momentum, polar and azimuthal angles (θ,ϕ)
  - RMS of fast smearing spectra
- Provides for reliable projections
  - Limitation: selection of hadronic state not implemented
  - Could provide better identification DIS events

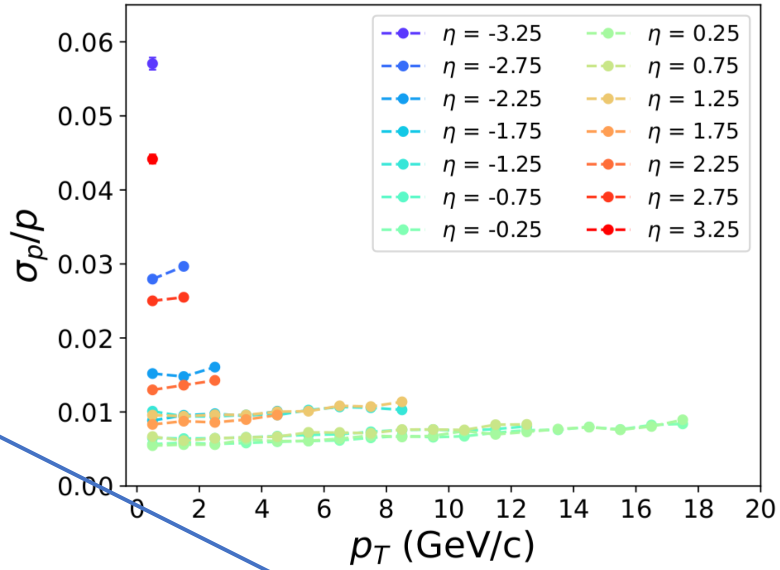

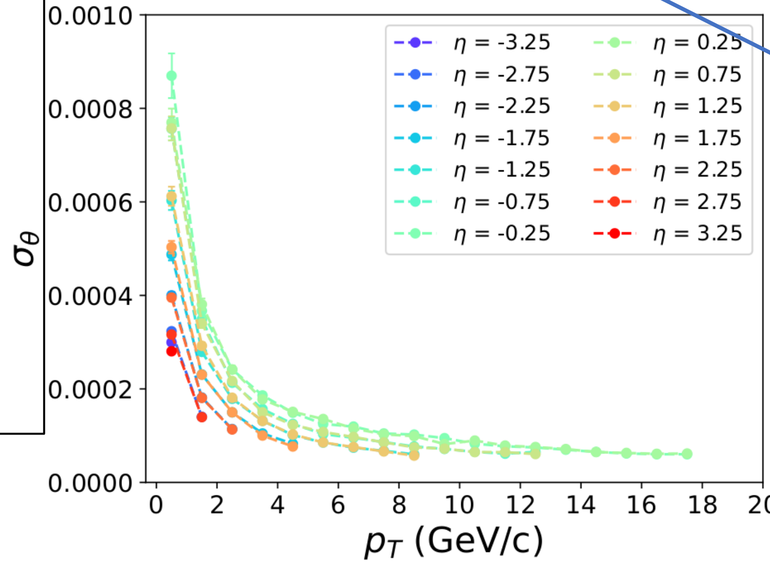

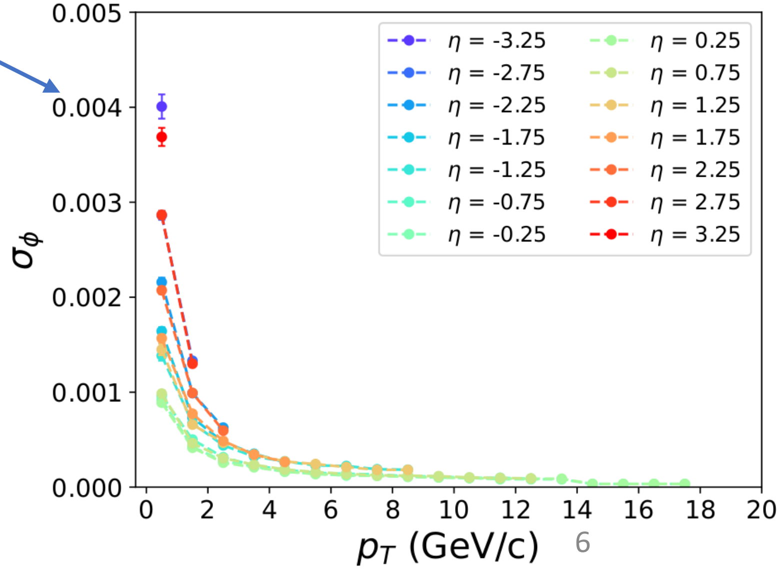

“unpolarized” PV

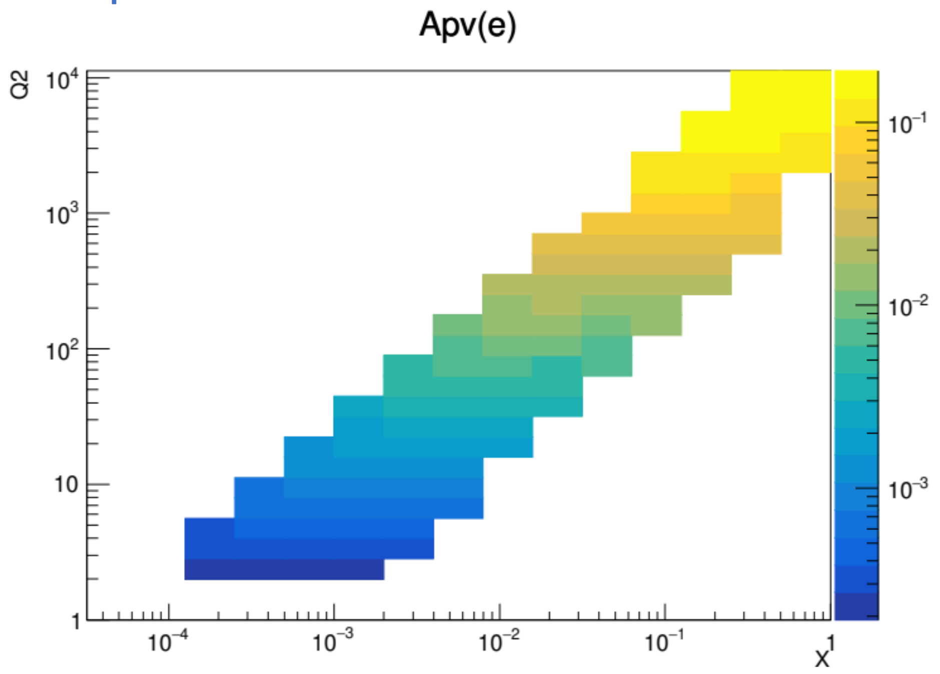

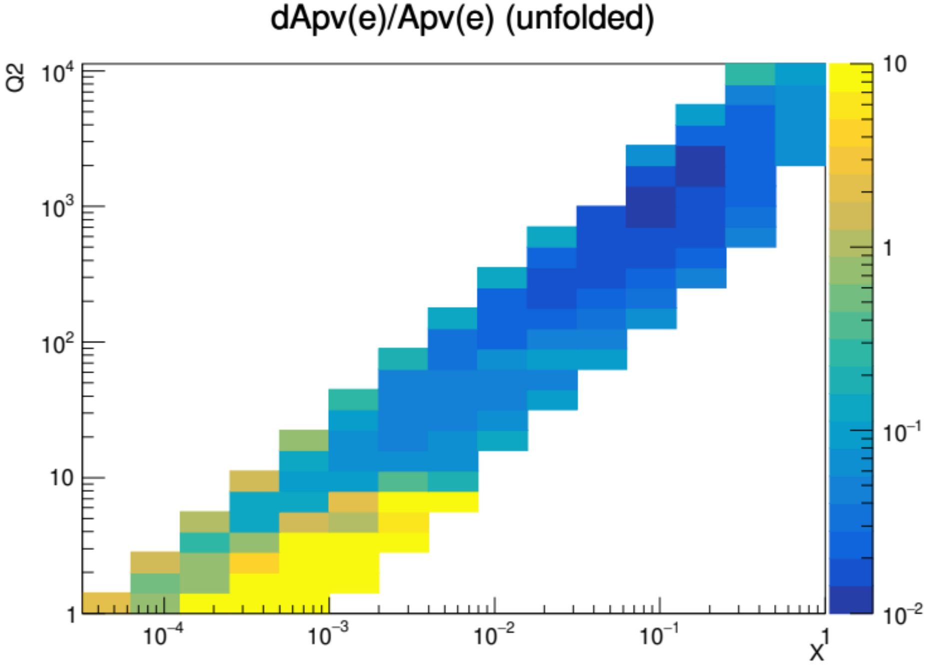

“polarized” PV

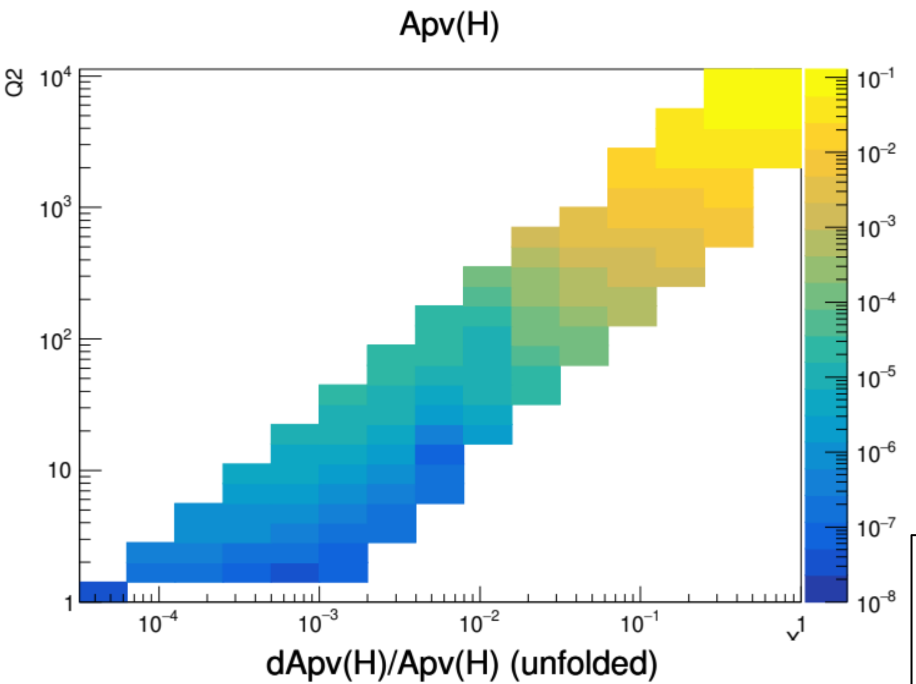

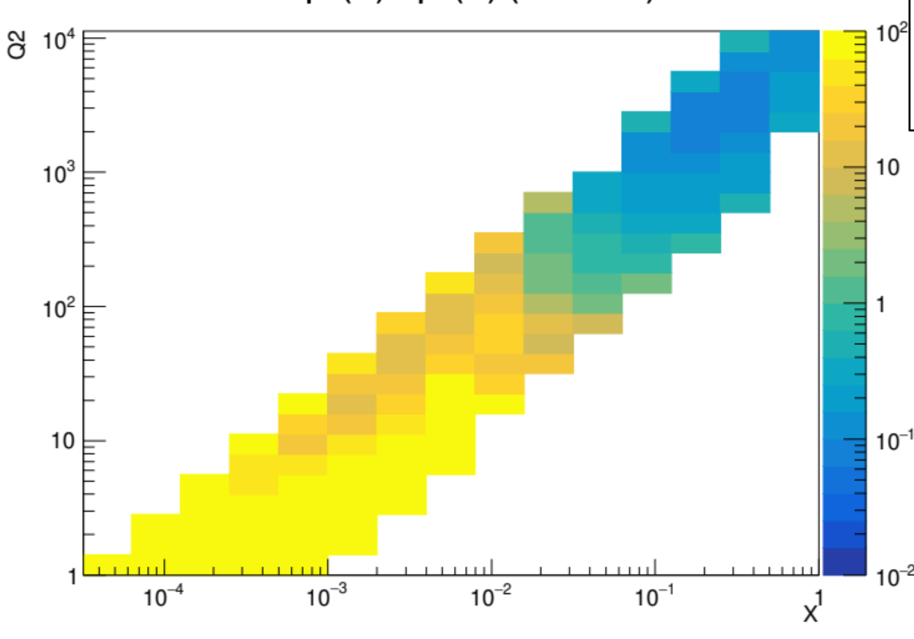

18x275 ep 100 fb^{-1}

Event selection applied

- $Q^2_{det}>1.0$ GeV
- $y_{det}>0.1$ & $y_{det}<0.9$
- $\eta_{det}>-3.5$ and $\eta_{det}<3.5$

“unpolarized” PV

“polarized” PV

18x275 ep 100 fb^{-1}

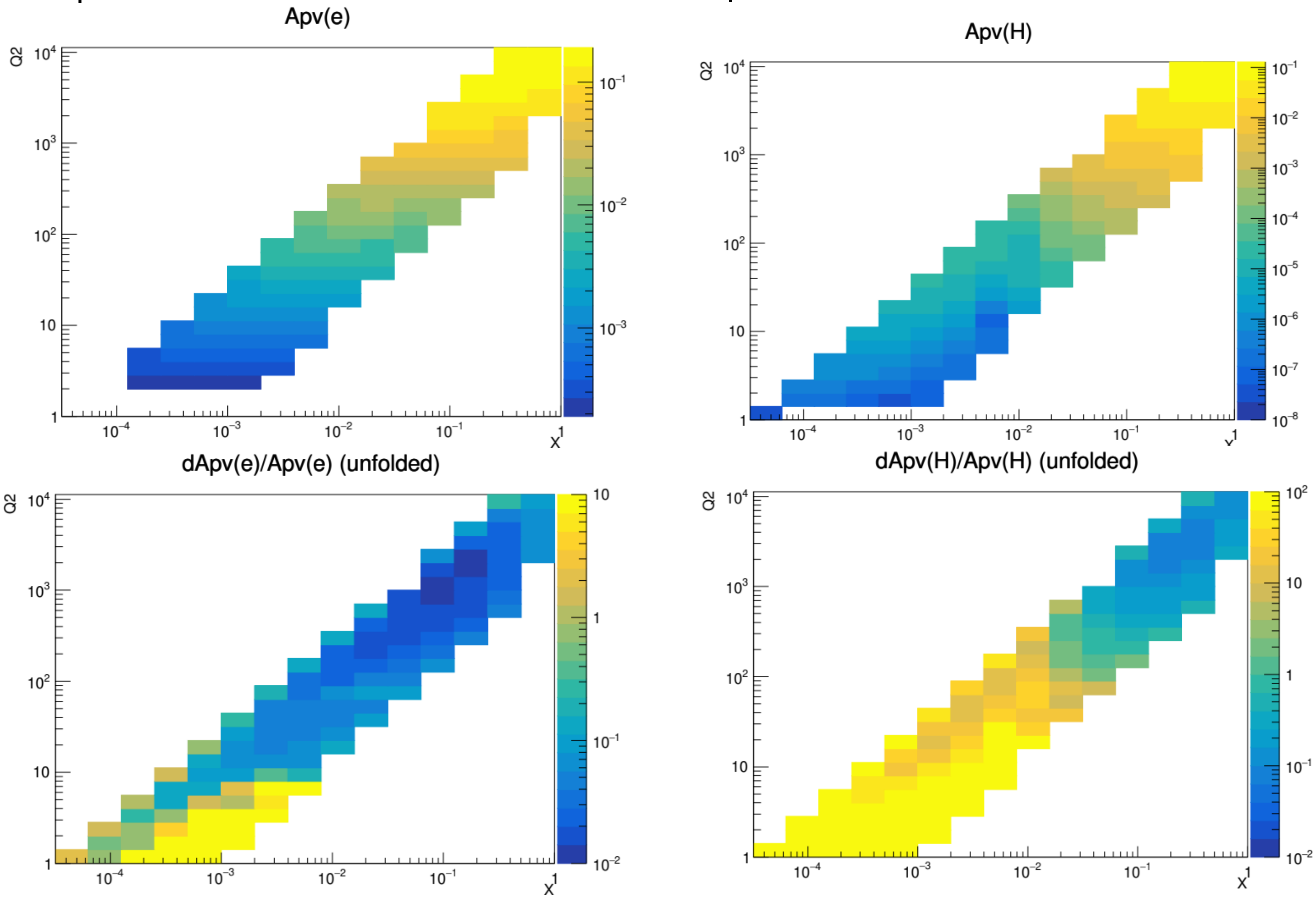

These also represent precision on the “additional EW structure functions” (namely $g_{1,5}^{\gamma Z}$)

Pseudo-Data & Uncertainties

Pseudo-Data Generation

- In each bin $(\sqrt{s}, Q^2, x)$
  - Nominal PDF set used to calculate A_{PV}^{theo}
  - Remaining PDF sets used to determine PDF uncertainty

$\sin^2\theta_W = 0.231$ used in generation of pseudo-data

- Generate pseudo-experimental asymmetry utilizing the statistical and systematic uncertainties

$$(A_{PV})_b^{pseudo} = (A_{PV})_{SM,b}^{theo} + r_b \underbrace{\sqrt{\sigma_{stat}^2 + \left[(A_{PV})_{SM,b}^{theo}\left(\frac{\sigma_{sys}}{A}\right)_b\right]^2}}_{\text{Uncorrelated uncertainties}} + r' \underbrace{\sqrt{\left[(A_{PV})_{SM,b}^{theo}\left(\frac{\sigma_{pol}}{A}\right)_b\right]^2}}_{\text{Correlated uncertainties}}$$

- r_b and r': random number drawn from Normal distribution
- r' common across all bins

Experimental Uncertainties

- Statistical: $dA_{stat}=\frac{1}{\sqrt{N}}$
- Systematics
  - Background: $\frac{\sigma_{bg}}{A} = 1\%$
  - Polarimetry: $\frac{\sigma_{pol}}{A} = 1\%$

    (e$^-$ beam polarization = 80%)

Diagonal Terms

$$\sigma_b^2 = \sigma_{\mathrm{stat},b}^2 + \left[(A_{\mathrm{PV}})_{\mathrm{SM},0,b}^{\mathrm{theo}}\left(\frac{\sigma_{\mathrm{sys}}}{A}\right)_b\right]^2 + \left[(A_{\mathrm{PV}})_{\mathrm{SM},0,b}^{\mathrm{theo}}\left(\frac{\sigma_{\mathrm{pol}}}{A}\right)_b\right]^2$$

Off-Diagonal Terms

$$\sigma_b = (A_{\mathrm{PV}})_{\mathrm{SM},0,b}^{\mathrm{theo}}\left(\frac{\sigma_{\mathrm{pol}}}{A}\right)_b$$

Experimental Uncertainty Matrix

$$\Sigma_0^2 = \begin{bmatrix} \sigma_1^2 & \sigma_1\sigma_2 & \cdots & \sigma_1\sigma_{N_{bin}} \\ & \sigma_2^2 & \cdots & \sigma_2\sigma_{N_{bin}} \\ & & \ddots & \vdots \\ & & & \sigma_{N_{bin}}^2 \end{bmatrix}$$

PDF Uncertainties

- PDF uncertainties were determined following the prescription of each PDF set (CT18NLO, MMHT2014, NNPDF31)
- Hessian

$$\left(\Sigma^2_{pdf}\right)_{bb'} = \frac{1}{4}\sum_{m=1}^{N_{pdf}/2}\left(A^{theo}_{SM,2m,b} - A^{theo}_{SM,2m-1,b}\right)\left(A^{theo}_{SM,2m,b'} - A^{theo}_{SM,2m-1,b'}\right)$$

- Replica

$$\left(\Sigma^2_{pdf}\right)_{bb'} = \frac{1}{N_{pdf}}\sum_{m=1}^{N_{pdf}}\left(A^{theo}_{SM,m,b} - A^{theo}_{SM,0,b}\right)\left(A^{theo}_{SM,m,b'} - A^{theo}_{SM,0,b'}\right)$$

Accounted for both diagonal and off-diagonal elements of PDF uncertainty

PDF Uncertainty Matrix

$$\Sigma^2_{pdf} = \begin{bmatrix} \sigma^2_{1,pdf} & \sigma_{1,pdf}\sigma_{2,pdf} & \cdots & \sigma_{1,pdf}\,\sigma_{N_{bin,pdf}} \\ & \sigma^2_{2,pdf} & \cdots & \sigma_2\sigma_{N_{bin,pdf}} \\ & & \ddots & \vdots \\ & & & \sigma^2_{N_{bin,pdf}} \end{bmatrix}$$

Extraction of the Weak Mixing Angle

$$A_{RL}^{e^-} = \frac{|\lambda|\eta_{\gamma Z}\left[g_A^e 2yF_1^{\gamma Z} + g_A^e\left(\frac{2}{xy} - \frac{2}{x} - \frac{2M^2xy}{Q^2}\right)F_2^{\gamma Z} + g_V^e(2-y)F_3^{\gamma Z}\right]}{2yF_1^{\gamma} + \left(\frac{2}{xy} - \frac{2}{x} - \frac{2M^2xy}{Q^2}\right)F_2^{\gamma} - \eta_{\gamma Z}\left[g_V^e 2yF_1^{\gamma Z} + g_V^e\left(\frac{2}{xy} - \frac{2}{x} - \frac{2M^2xy}{Q^2}\right)F_2^{\gamma Z} + g_A^e(2-y)F_3^{\gamma Z}\right]}$$

- Extraction of $\sin^2\theta_W$ from minimization of the χ^2

$$\chi^2 = [A^{pseudo-data} - \boldsymbol{A^{theory}}]^T(\Sigma^2)^{-1}[A^{pseudo-data} - \boldsymbol{A^{theory}}]$$

- A^{theory} is a function of $\sin^2\theta_W$ via the weak neutral couplings: $A^{theory}(\boldsymbol{\sin^2\theta_W})$
- Single parameter fit to extract → $\boldsymbol{\sin^2\theta_W}$

Uncertainty Matrix

$$(\Sigma^2)_{bb'} = (\Sigma_0^2)_{bb'} + \left(\Sigma_{pdf}^2\right)_{bb'}$$

Fitting of weak mixing angle

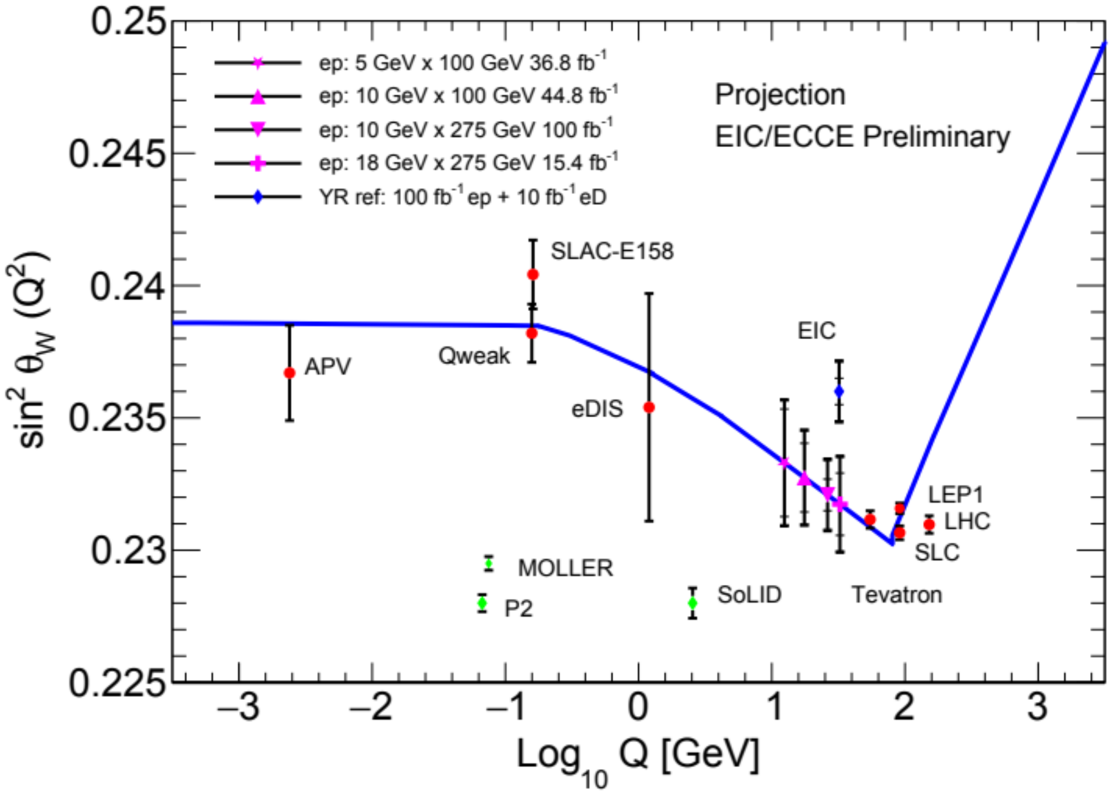

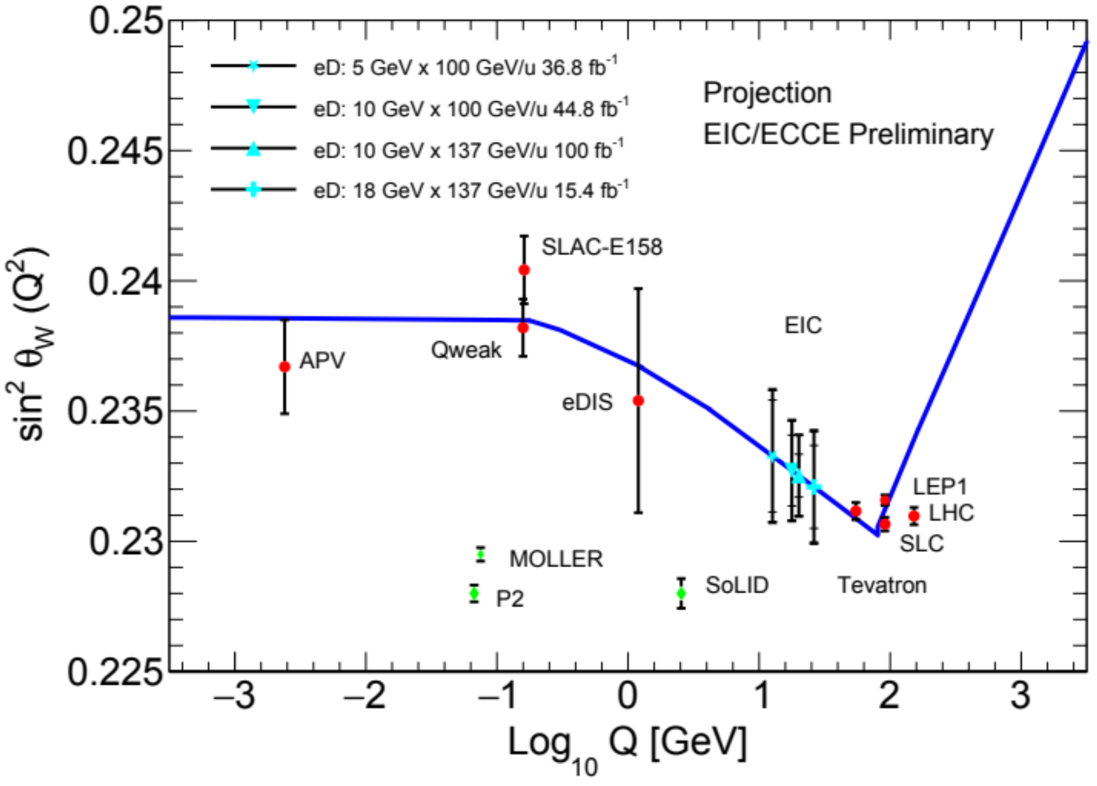

Take-way: ep better than eD; statistical and beam polarimetry uncertainties dominate; PDF uncertainty not a big issue; moderate precision in an unmeasured energy region, multi-year run would help

Summary of Results

ep Results

EIC Yellow Report Setting ↓

Beam type and energy Label	ep 5 × 100 P2	ep 10 × 100 P3	ep 10 × 275 P4	ep 18 × 275 P5	ep 18 × 275 P6
Luminosity (fb^{-1})	36.8	44.8	100	15.4	(100 YR ref)
$\langle Q^2 \rangle$ (GeV^2)	154.4	308.1	687.3	1055.1	1055.1
$\langle A_{PV} \rangle$ ($P_e = 0.8$)	−0.00854	−0.01617	−0.03254	−0.04594	−0.04594
$(dA/A)_{\text{stat}}$	1.54%	0.98%	0.40%	0.80%	(0.31%)
$(dA/A)_{\text{stat+syst(bg)}}$	1.55%	1.00%	0.43%	0.81%	(0.35%)
$(dA/A)_{1\%\text{pol}}$	1.0%	1.0%	1.0%	1.0%	(1.0%)
$(dA/A)_{\text{tot}}$	1.84%	1.42%	1.09%	1.29%	(1.06%)
Experimental					
$d(\sin^2\theta_W)_{\text{stat+syst(bg)}}$	0.002032	0.001299	0.000597	0.001176	0.000516
$d(\sin^2\theta_W)_{\text{stat+syst+pol}}$	0.002342	0.001759	0.001297	0.001769	0.001244
with PDF					
$d(\sin^2\theta_W)_{\text{tot,CT18NLO}}$	0.002388	0.001807	0.001363	0.001823	0.001320
$d(\sin^2\theta_W)_{\text{tot,MMHT2014}}$	0.002353	0.001771	0.001319	0.001781	0.001270
$d(\sin^2\theta_W)_{\text{tot,NNPDF31}}$	0.002351	0.001789	0.001313	0.001801	0.001308

eD Results

Beam type and energy Label	eD 5 × 100 D2	eD 10 × 100 D3	eD 10 × 137 D4	eD 18 × 137 D5	eD 18 × 137 N/A
Luminosity (fb^{-1})	36.8	44.8	100	15.4	(10 YR ref)
$\langle Q^2 \rangle$ (GeV^2)	160.0	316.9	403.5	687.2	687.2
$\langle A_{PV} \rangle$ ($P_e = 0.8$)	−0.01028	−0.01923	−0.02366	−0.03719	−0.03719
$(dA/A)_{\text{stat}}$	1.46%	0.93%	0.54%	1.05%	(1.31%)
$(dA/A)_{\text{stat+bg}}$	1.47%	0.95%	0.56%	1.07%	(1.32%)
$(dA/A)_{\text{syst,1\%pol}}$	1.0%	1.0%	1.0%	1.0%	(1.0%)
$(dA/A)_{\text{tot}}$	1.78%	1.38%	1.15%	1.46%	(1.66%)
Experimental					
$d(\sin^2\theta_W)_{\text{stat+bg}}$	0.002148	0.001359	0.000823	0.001591	0.001963
$d(\sin^2\theta_W)_{\text{stat+bg+pol}}$	0.002515	0.001904	0.001544	0.002116	0.002414
with PDF					
$d(\sin^2\theta_W)_{\text{tot,CT18}}$	0.002558	0.001936	0.001566	0.002173	0.00247
$d(\sin^2\theta_W)_{\text{tot,MMHT2014}}$	0.002527	0.001917	0.001562	0.002128	0.002424
$d(\sin^2\theta_W)_{\text{tot,NNPDF31}}$	0.002526	0.001915	0.001560	0.002127	0.002423

*Tables from: https://arxiv.org/pdf/2204.07557.pdf *

Take-way: ep better than eD; **statistical and beam polarimetry uncertainties dominate**; PDF uncertainty not a big issue; moderate precision in an unmeasured energy region, multi-year run would help

Conclusion

- We preformed a detailed study of the extraction of $\sin^2\theta_W$ at the EIC using the ECCE detector design for both the proton and deuteron
  - Accounted for statistical, systematic, and PDF uncertainties and relevant correlations (i.e. PDF)
  - Overall uncertainties larger than those in Yellow Report
- Statistical and beam polarimetry uncertainties dominate
- The EIC can play an important role in Electroweak and BSM physics covering energy scale between fixed target and collider experiments

Thank You

Data sets simulated and processed:

D1	5 GeV $\times$ 41 GeV eD, 4.4 fb^{-1}	P1	5 GeV $\times$ 41 GeV ep, 4.4 fb^{-1}
D2	5 GeV $\times$ 100 GeV eD, 36.8 fb^{-1}	P2	5 GeV $\times$ 100 GeV ep, 36.8 fb^{-1}
D3	10 GeV $\times$ 100 GeV eD, 44.8 fb^{-1}	P3	10 GeV $\times$ 100 GeV ep, 44.8 fb^{-1}
D4	10 GeV $\times$ 137 GeV eD, 100 fb^{-1}	P4	10 GeV $\times$ 275 GeV ep, 100 fb^{-1}
D5	18 GeV $\times$ 137 GeV eD, 15.4 fb^{-1}	P5	18 GeV $\times$ 275 GeV ep, 15.4 fb^{-1}
		P6	18 GeV $\times$ 275 GeV ep, 100 fb^{-1}